OPTICAL AND PHOTOCATALYTIC PROPERTIES OF ELECTROSPUN ZnO FIBERS

C. BUSUIOC[a, b*], A. EVANGHELIDIS[a], M. ENCULESCU[a], I. ENCULESCU[a]
[a]*National Institute of Materials Physics, RO-077125, Magurele, Romania*
[b]*University "Politehnica" of Bucharest, RO-011061, Bucharest, Romania*

ZnO nanofibers were obtained by electrospinning a solution of zinc acetate dihydrate and polyvinylpyrrolidone in N,N-dimethylformamide, followed by calcination at 500, 650 or 800 °C for 1 h. X-ray diffraction, selected area electron diffraction, scanning electron microscopy, transmission electron microscopy, reflectance spectroscopy and photoluminescence spectroscopy were used for the characterization of the resulting fibers. The thermally treated samples exhibit ZnO single phase with polycrystalline hexagonal structure. The morphological investigation revealed an accentuated contraction process during calcination, as well as the increase of the crystallite size and the appearance of a breaking tendency with the calcination temperature enhancement. Both UV and Visible emissions under excitation at 350 nm were showed by the optical studies, which also led to band gap values slightly lower than those reported for similar one-dimensional nanostructures. In order to assess the photocatalytic activity of ZnO fibers, the photodegradation of methylene blue in aqueous medium (10^{-3} M) under UV irradiation (368 nm) was analyzed.

1. Introduction

Zinc oxide (ZnO), a material studied for more than 80 years, exhibits appealing properties for the fields of electronics, optoelectronics, spintronics or photovoltaics [1, 2]. If a few decades ago the scientific research was focused mainly on bulk related topics, nowadays the emphasis is essentially on nanostructures synthesis and characterization. The spectacular revival of ZnO domain during the past 20 years can be explained by the development of novel growth methods which lead to exotic morphologies, new doping techniques that promote remarkable properties or advanced investigation facilities which allow a better understanding of some intrinsic mechanisms. Moreover, the interest of the researchers gradually shifted towards the design and fabrication of applications with improved features.

ZnO has a wide direct bandgap (3.3 eV) and crystallises in the hexagonal wurtzite type structure [3]. Several studies showed that ZnO is the second most studied semiconductor material, since it represents an alternative to traditional materials, such as silicon or gallium nitride [4]. In addition, it is a cheap and transparent semiconducting oxide that can be easily integrated in devices like transistors, diodes, lasers, sensors or solar cells [5-12]. However, the main advantages of this oxide consist of its availability, polymorphism and scalability. Thus, starting from a wide variety of zinc sources, ZnO can be easily prepared in the form of powders, fibers, films or bulk bodies by using different physical [13], chemical [14] or electrochemical [15] methods.

In this context, ZnO one-dimensional nanostructures, such as belts [16], fibers [17-21], wires [22] or rods [11], are a suitable choice for the development of applications with superior properties due to the high surface to volume ratio, modified surface energy and potential size effects [23]. One of the most simple and inexpensive methods to get fibers is electrospinning [24-

---

*Corresponding author: cristina.busuioc@infim.ro

28], a technique that has become extremely popular in recent years due to its capability to produce polymeric, metallic or ceramic fibers starting from a solution with certain viscoelastic properties. Thus, the precursor solution is pumped at a constant rate under a high electric field, the resulting fiber being gathered on a collector that is placed at a certain distance from the spinneret. Usually, the diameter of the fibers synthesized in this manner ranges between tens of nanometers and several micrometers. Furthermore, by modifying the collector geometry and the deposition conditions, nonwoven mesh or well aligned arrays with different thickness can be obtained.

Recently, semiconductor materials, like TiO_2 ZnO or SnO_2, have attracted increasing attention for their photocatalytic properties, which can be exploited for environmental related applications. Thus, many papers reported that ZnO can be efficient in photocatalytic degradation of some organic dyes [29-32], the main factors affecting its performances being the specific surface area, the irradiation light absorption and the separation efficiency of electron-hole pairs [33]. Furthermore, it was shown that the material morphology plays a crucial role for ZnO photocatalysts [34], the enhancement of the surface area being a suitable approach.

In this work, ZnO fibers were fabricated via the electrospinning technique. In order to remove the carrier polymer and promote the oxide crystallization, the precursor fibers were calcined at temperatures in the 500 - 800 °C range. Furthermore, the influence of the processing parameters on the morphological and optical properties of the resulting fibers was studied. The photocatalytic activity of ZnO fibers was estimated by performing preliminary tests for the degradation of methylene blue aqueous solution under UV irradiation.

2. Experimental procedure

ZnO fibers were prepared by the electrospinning technique, using a lab made setup. Zinc acetate dihydrate ($Zn(Ac)_2 \cdot 2H_2O$, Sigma-Aldrich, ≥98%), polyvinylpyrrolidone (PVP, MW = 1.300.000, Sigma-Aldrich) and N,N-dimethylformamide (DMF, ≥99,8%, Sigma-Aldrich) were used as starting materials. First, 2 g of $Zn(Ac)_2 \cdot 2H_2O$ were dissolved in 5 mL DMF with stirring for 1 h at 50 °C. Then, 1 g of PVP was added, the resulting solution being stirred for 10 h at 50 °C. A colourless solution was obtained. Further, the precursor solution was electrospun in optimized conditions: a voltage of 25 kV, a feeding rate of 0.1 mL/h and a distance of 17 cm between the spinneret and the collector. Silicon plates were employed as substrates. In order to promote the crystallisation of ZnO phase, the as-spun fibers were calcined for 1 h at 500, 650 or 800 °C, in air, with a heating rate of 1 °C/min.

ZnO fibers were investigated by thermal analysis (DTA-TG), X-ray diffraction (XRD), scanning electron microscopy (SEM), selected area electron diffraction (SAED), transmission electron microscopy (TEM), reflectance spectroscopy (RS) and photoluminescence spectroscopy (PL). The thermal analysis was performed on a Shimadzu DTG-60 equipment, in the 20 - 1000 °C temperature range, in air. A PANalytical Empyrean diffractometer with Cu Kα radiation ($\lambda = 0.154$ nm) was used to identify the phase composition and crystal structure of the calcined fibers, 2θ ranging between 20 and 80 ° and the incidence angle being set at 0.5 °. The average crystallite size (D) was calculated using Scherrer equation: $D=K \cdot \lambda/(\beta \cdot cos\theta)$, where K is a dimensionless shape factor with a typical value of about 0.9, λ is the X-ray wavelength (0.154nm), β is the full width at half maximum (FWHM) value corresponding to (101) diffraction peak and θ is Bragg angle. An Evo 50 XVP scanning electron microscope and a Tecnai G^2 F-30 S-Twin transmission electron microscope with selected area electron diffraction (SAED) facility were employed to visualize the samples morphology. The reflectance spectra were recorded with a Perkin-Elmer Lambda 45 UV-Vis spectrophotometer and the photoluminescence spectra with a FL 920 Edinburgh Instruments spectrophotometer. In order to estimate the band gap values, Kubelka-Munk functions (F(R)) were calculated using the reflectance data and $[F(R) \cdot E]^{1/2}$ functions were plotted versus photon energy (E); Kubelka-Munk function is expressed as $F(R)=(1-R)^2/(2 \cdot R)$, where R is the observed diffuse reflectance. An ULVAC-RIKO PCC2 Photocatalysis Evaluation Checker was employed to assess the photocatalytic activity of ZnO fibers prepared via electrospinning, methylene blue in aqueous solution being udes as test dye; the intensity of a 610 nm beam emitted by the samples surface (1x2 cm^2) within 1 hour was studied.

3. Results and discussion

In order to study ZnO fiber formation mechanism and to identify the appropriate calcination temperatures, the as-spun fibers were subjected to thermal analysis from room temperature to 1000 °C, the results being displayed in Fig. 1a. The thermogravimetric data indicate a weight loss of about 73% in the 25 - 500 °C temperature range, divided in three major steps. The endothermic effect below 200 °C corresponding to 11.2 % weight loss is assigned to the loss of solvent and moisture, as well as $ZnAc_2 \cdot H_2O$ dehydration. The second weight loss (32.0 %), associated with a minor exothermic effect corresponds to $ZnAc_2$ decomposition. The strong and complex exothermic effect with maximum at 440 °C and 29.8 % weight loss is attributed to PVP degradation and ZnO crystallisation. Above 500 °C no other weight loss is noticed, meaning that the organic part is completely removed at this temperature. In comparison with the thermal behavior of each raw material considered separately, some of the thermal effects are shifted to higher or lower temperatures, indicating some interactions between the acetate and PVP. As it can be seen in Fig. 1b, the precursor fibers are randomly oriented, but continuous and smooth; they have an average diameter of about 200 nm. Moreover, the density of the fiber web can be easily adjusted by controlling the deposition time. As well, by varying the deposition parameters (voltage, distance between spinneret and collector etc.), thinner or thicker fibers can be obtained, such that the morphological properties of the resulting web are tunable and satisfy the requirements of various applications.
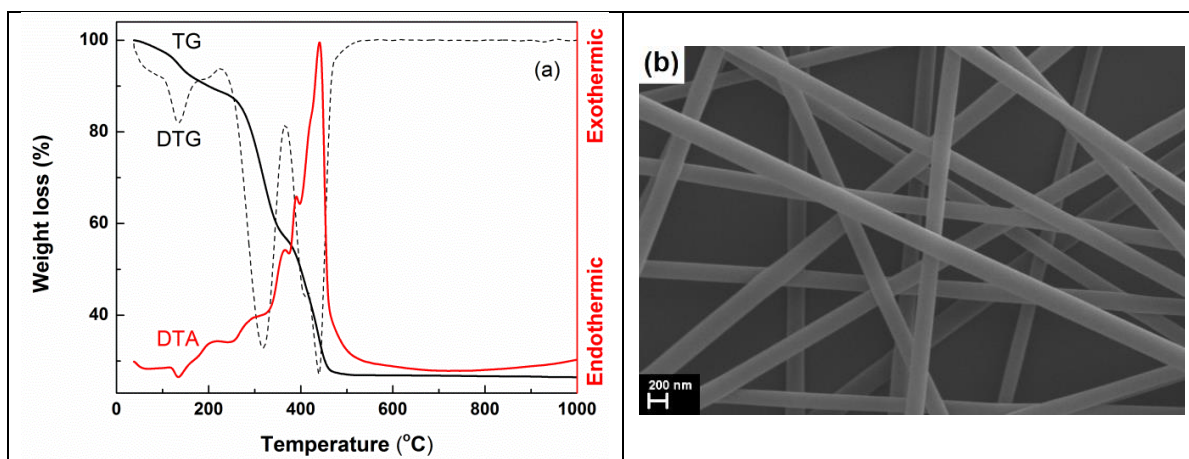

Fig. 1. Thermal analysis (a) and SEM image (b) of the precursor fibers.

The crystalline phases of the thermally treated fibers were identified by XRD. Fig. 2 presents the X-ray diffractograms of ZnO fibers calcined at three different temperatures. All samples exhibit sharp and narrow diffraction peaks, assigned to ZnO single phase with hexagonal wurtzite structure (JCPDS 04-006-7189). As expected, the increase of the calcination temperature promotes the crystallite growth, the average values calculated with Scherrer equation being 25 nm (500 °C), 34 nm (650 °C) and 37 nm (800 °C), respectively. Thus, highly crystalline ZnO fibers can be produced even for the lowest calcination temperature, in the case of which the average crystallite size is the smallest.
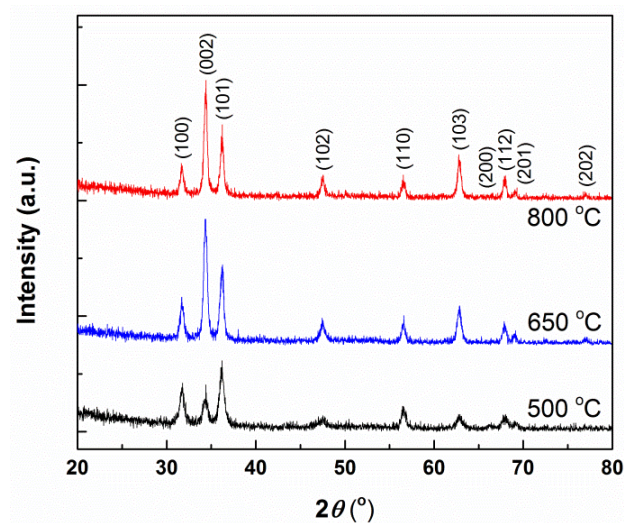
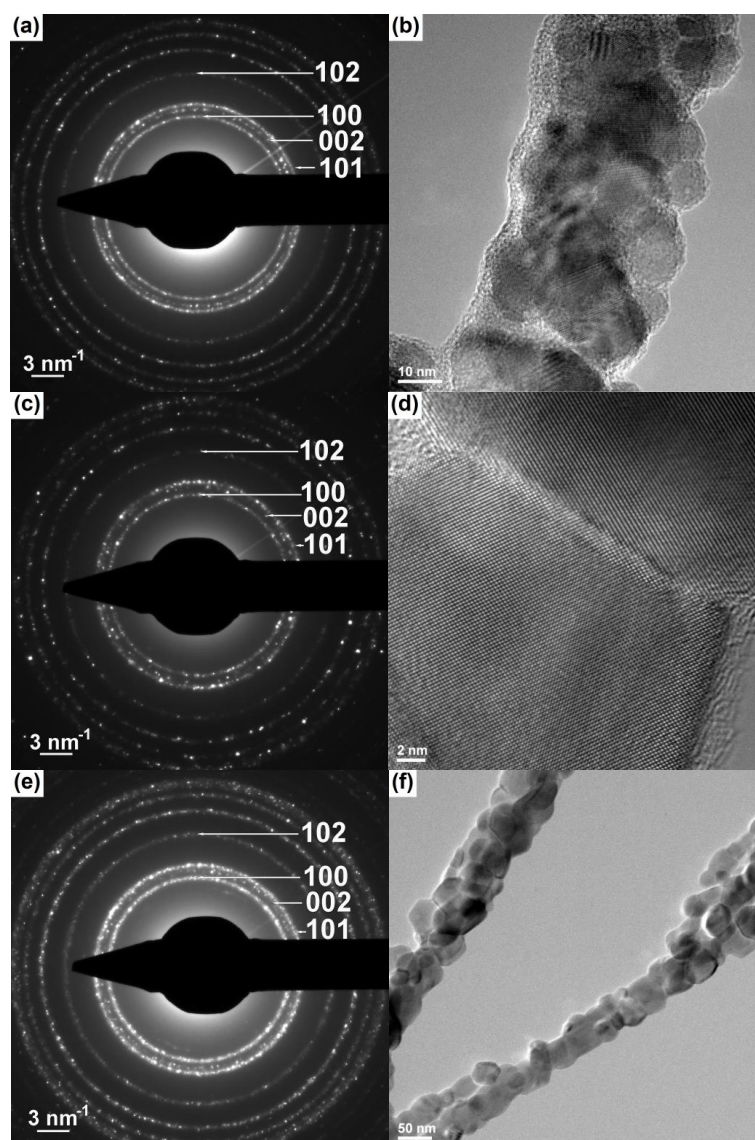*Fig. 2. XRD patterns of ZnO fibers calcined at different temperatures.*

Further, the morphology of the resulting fibers was visualized by SEM. Fig. 3 displays SEM images at low or high magnification of ZnO fibers calcined at different temperatures. It is obvious that the thermal treatment significantly changes the morphological properties of the as-spun material. The calcined fibers are no longer smooth, their surface becoming rather rough due to the burning of the carrier polymer, followed by the crystallization of an oxide phase in the form of nanometric grains. Considering the average diameter of the fibers before and after the thermal treatment, it can be stated that the one-dimensional structures undergo a contraction process, which leads to size values two - three times lower (below 100 nm) for all three experimental temperatures. Moreover, the increase of the calcination temperature from 500 to 800 °C is accompanied by an accentuated tendency of breaking, such that the sample thermally treated at the highest temperature consists of a mixture of fibers with various lengths. The phenomenon of fiber disintegration, already reported in the scientific literature, is driven by the so-called Rayleigh instability, in the case of which the morphology transformation process is influenced by the annealing time and temperature [35].
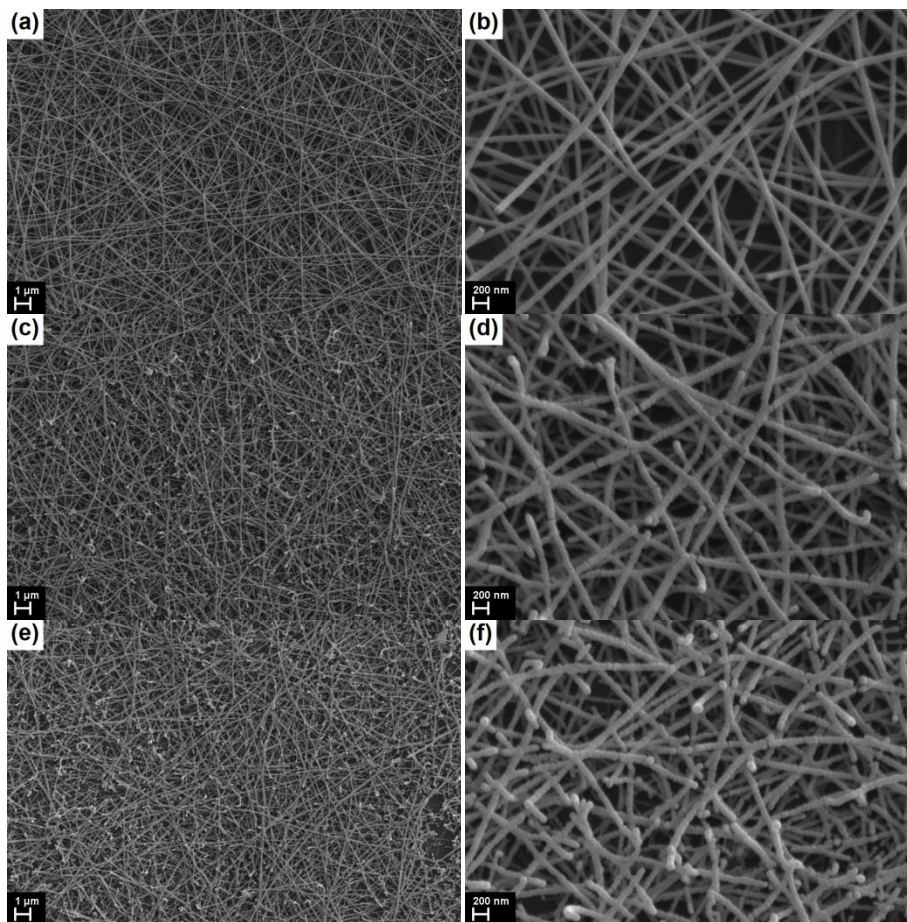
Fig. 3. SEM images of ZnO fibers calcined at 500 °C (a and b), 650 °C (c and d)
and 800 °C (e and f).

In order to get a more detailed image of the oxide fibers obtained via electrospinning, SAED and TEM investigations were used, the results being shown in Fig. 4. Thus, the SAED patterns indicate the polycrystalinity of ZnO fibers calcined at different temperatures and confirm their hexagonal structure through the main diffraction rings of ZnO single phase. The TEM images of the samples thermally treated at 500 or 800 °C reveal the existence of some very thin fibers, with diameter values below 50 nm, as well as the increase of the crystallite size with the calcination temperature enhancement; if in the first case one can find two or three crystallites on a cross-section of the fiber, in the second one the fiber diameter may coincide with the crystallite diameter. Regarding the HRTEM image of the sample thermally treated at 650 °C, a crystallite boundary, as well as different crystalline planes can be well observed; as well, the crystallites seem to be surrounded by an amorphous layer with a thickness of about 2 nm.

*Fig. 4. SAED pattern (a) and TEM image (b) of ZnO fibers calcined at 500 °C, SAED
pattern (c) and HRTEM image (d) of ZnO fibers calcined at 650 °C and SAED pattern
(e) and TEM image (f) of ZnO fibers calcined at 800 °C.*

The optical properties of ZnO fibers were also investigated. The reflection spectra of all prepared samples exhibit a pronounced decrease of the reflectance between 370 and 380 nm (Fig. 5a), process that can be associated with the band to band transition in ZnO. The band gap values calculated with Kubelka-Munk function are 3.05 eV (500 °C), 3.15 eV (650 °C) and 3.16 eV (800 °C), respectively (Fig. 5b), values that are slightly lower than those reported in the scientific literature for different ZnO nanostructures [14, 15, 26, 36]. Taking into account the trend of the average crystallite size with the increase of the calcination temperature, the band gap shift could be attributed to a size effect.

In respect to the photoluminescence properties, it is well known that a typical spectrum of ZnO exhibits a near band edge UV emission due to free exciton transitions and a broad deep level visible (green-yellow) emission, which depends on the intrinsic defects, such as oxygen vacancy, zinc vacancy, interstitial oxygen, interstitial zinc and antisite oxygen, other than crystalline defects, like dislocations or grain boundaries [37]. Fig. 6a presents the photoluminescence spectra of ZnO fibers for an excitation wavelength of 350 nm. The intensity of the emission bands rises with the increase of the calcinations temperature from 500 to 800 °C, which could be related to

crystallite size, surface area and defects concentration evolution. Thus, the UV peak with maximum at around 380 nm is attributed to the band to band recombination [37], while the broad visible band could be deconvoluted into several components; the green emission with maximum at around 530 nm corresponds to oxygen vacancies [22], the blue emission (between 400 and 500 nm) is associated with zinc vacancies or interstitials [38] and the yellow and orange ones (above 550 nm) are explained by the excess oxygen [39].
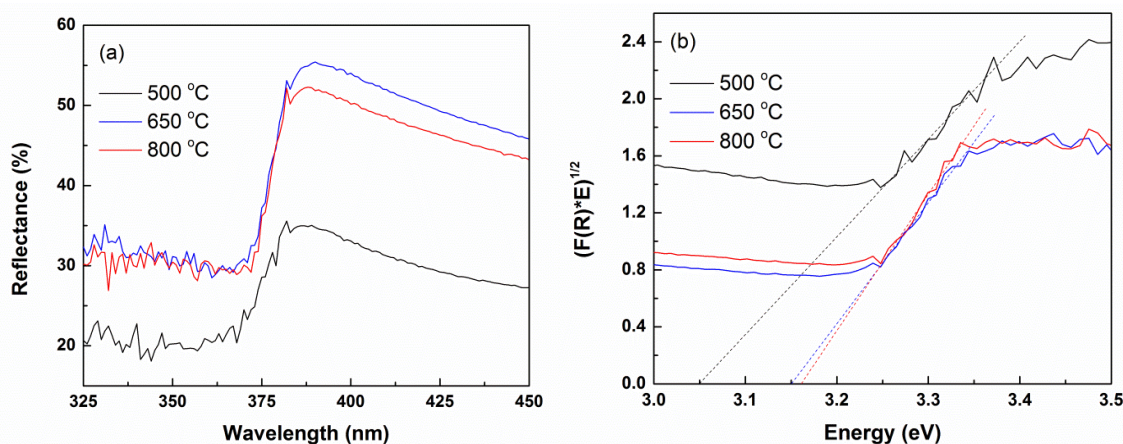

Fig. 5. Reflectance spectra (a) and representation of Kubelka-Munk functions (b) for ZnO fibers calcined at different temperatures.

In order to estimate the pollutant degradation capability of ZnO fibers prepared via electrospinning, photodegradation of methylene blue aqueous solution under UV irradiation was examined. First, the samples were cleaned by UV irradiation, afterwards impregnated with a 10^{-3} M dye solution and dried, thereupon measured under irradiation at 368 nm. As is can be seen in Fig. 6b, the sample calcined at 500 °C exhibits the best photocatalytic behaviour, the corresponding curve showing no saturation tendency after 60 min of operating, as against the other two curves which seems to reach maximum values of 1.5 (red curve) and 2 % (blue curve), respectively. Indeed, a photodegradation capability of not more than 3.5 % (black curve) is a modest result in comparison with other papers [29, 32, 40], but if we take into account that the analyzed surface was covered with an extremely thin layer of fibers (few tens of fibers arranged one above the other in a random way), among which there are many empty spaces, and the dye concentration is higher than the one typically used for such research studies (10^{-5}-10^{-6}), the outcome can be viewed in a different light. Moreover, ZnO fibers thermally treated at the lowest temperature may be tested for a longer time, so as to achieve saturation. As well, it can be stated that the average crystallite size and the optical characteristics strongly influence the photocatalytic activity of the fabricated oxide fibers.
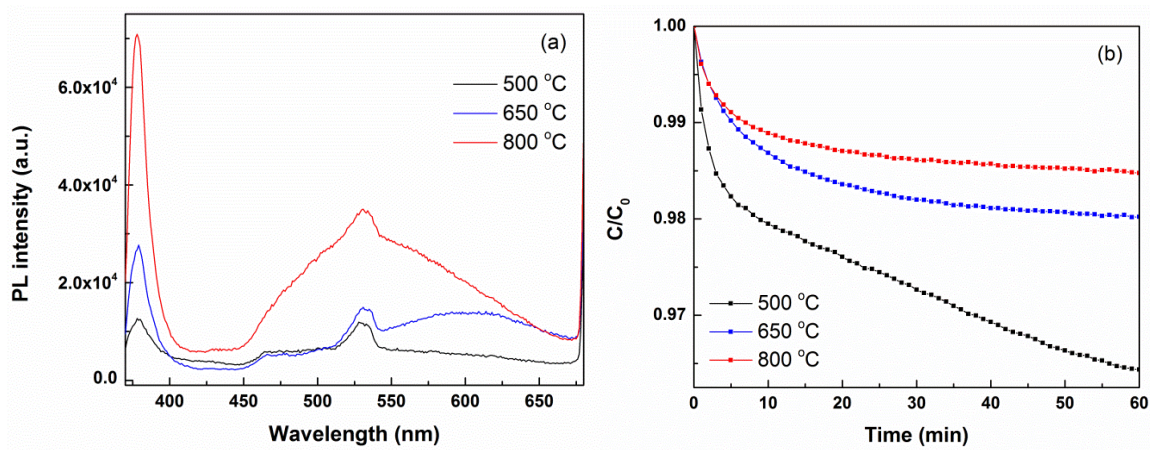
Fig. 6. PL spectra (a) and photocatalytic degradation curves of methylene blue under
UV irradiation for ZnO fibers calcined at different temperatures.

4. Conclusions

ZnO nanofibers were successfully prepared via the electrospinning technique. The precursor fibers were calcined at different temperatures in order to provide polymer burning and ZnO crystallisation in hexagonal phase. Regarding the diameter of the resulting fibers, the values are below 100 nm, compared to an average fiber diameter of 200 nm before the thermal treatment. The increase of the calcination temperature leads to crystallite size and band gap enhancement. All samples exhibit both excitonic and defects bands when excited at 350 nm, the evolution of point defects concentration being associated with the thermal treatment parameters. The photocatalytic activity of ZnO fibers was tested for a methylene blue aqueous solution (10^{-3} M) under UV irradiation (368 nm).

References

[1] F. Rahman; Nanostructures in Electronics and Photonics; Pan Stanford Publishing, Singapore, 2008.
[2] N.H. Nickel, E. Terukov; Zinc Oxide - A Material for Micro- and Optoelectronic Applications; Spinger, Netherlands, 2005.
[3] C. Klingshirn; ZnO: Material, Physics and Applications; ChemPhysChem **8,** 782 (2007).
[4] B.G. Svensson, S.J. Pearton, C. Jagadish; Semiconductors and Semimetals, **88**, Oxide Semiconductors; Academic Press, Elseier, USA, 2013.
[5] X. Wang, G. Zheng, G. He, J. Wei, H. Liu, Y. Lin, J. Zheng, D. Sun; Materials Letters **109,** 58 (2013).
[6] J.Y. Park, J.J. Kim, S.S. Kim; Electrical Transport Properties of ZnO Nanofibers; Microelectronic Engineering **101,** 8 (2013).
[7] Y. Feng, W. Hou, X. Zhang, P. Lv, Y. Li, W. Feng; Highly Sensitive Reversible Light-Driven

The Journal of Physical Chemistry C **115,** 3956 (2011).

[8] A. Katoch, G.J. Sun, S.W. Choi, J.H. Byun, S.S. Kim; Sensors and Actuators B **185,** 411 (2013).

[9] L. Liu, S. Li, J. Zhuang, L. Wang, J. Zhang, H. Li, Z. Liu, Y. Han, X. Jiang, P. Zhang; Sensors and Actuators B **155,** 782 (2011)–788.

[10] N. Horzum, D. Tascıoğlu, S. Okur, M.M. Demir; Talanta **85,** 1105 (2011).

[11] L. Song, P. Du, J. Xiong, F. Ko, C. Cui; Electrochimica Acta **163,** 330 (2015).

[12] P. Du, L. Song, J. Xiong, N. Li, Z. Xi, L. Wang, D. Jin, S. Guo, Y. Yuan; Electrochimica Acta **78,** 392 (2012).

[13] C. Cachoncinlle, C. Hebert, J. Perriere, M. Nistor, A. Petit, E. Millon; Applied Surface Science **336,** 103 (2015).

[14] N. Preda, M. Enculescu, I. Enculescu; Materials Letters **115**, 256 (2014).

[15] C. Florica, E. Matei, A. Costas, M.E. Toimil Molares, I. Enculescua; Electrochimica Acta **137,** 290 (2014).

[16] L. Yu, S. Liu, B. Yang, J. Wei, M. Lei, X. Fan; Materials Letters **141,** 79 (2015).

[17] W. Tang, J. Wang, P. Yao, X. Li; Sensors and Actuators B **192,** 543 (2014).

[18] S.S. Mali, H. Kim, W.Y. Jang, H.S. Park, P.S. Patil, C.K. Hong; ACS Sustainable Chemistry and Engineering **1**, 1207 (2013).

[19] C. Li, X. Zhang, W. Dong, Y. Liu; Materials Letters **80,** 145 (2012).

[20] Y. Wu, Z. Dong, N.J. Jenness, R.L. Clark; Materials Letters **65,** 2683 (2011).

[21] B. Ding, T. Ogawa, J. Kim, K. Fujimoto, S. Shiratori; Thin Solid Films **516,** 2495 (2008).

[22] S. Chakraborty, C.S. Tiwary, P. Kumbhakar; Journal of Physics and Chemistry of Solids **78,** 84 (2015).

[23] Q. Zhang, K. Zhang, D. Xu, G. Yang, H. Huang, F. Nie, C. Liu, S. Yang; Progress in Materials Science **60,** 208 (2014).

[24] S. Ramakrishna, K. Fujihara, W.E. Teo, T.C. Lim, Z. Ma; An Introduction to Electrospinning and Nanofibers; World Scientific Publishing, Singapore, 2005.

[25] J.H. Baek, J. Park, J. Kang, D. Kim, S.W. Koh, Y.C. Kang; Bulletin of the Korean Chemical Society **33,** 2694 (2012).

[26] H. Ren, Y. Ding, Y. Jiang, F. Xu, Z. Long, P. Zhang; Journal of Sol-Gel Science and Technology **52,** 287 (2009).

[27] J.A. Park, J. Moon, S.J. Lee, S.C. Lim, T. Zyung; Current Applied Physics **9**, S210 (2009).

[28] H. Wu, W. Pan; Journal of the American Ceramic Society **89**, 699 (2006).

[29] P. Singh, K. Mondal, A. Sharma; Journal of Colloid and Interface Science **394,** 208 (2013).

[30] F. Kayaci, C. Ozgit-Akgun, I. Donmez, N. Biyikli, T. Uyar; ACS Applied Materials and Interfaces **4,** 6185 (2012).

[31] K. Vignesh, M. Rajarajan, A. Suganthi; Journal of Industrial and Engineering Chemistry **20,** 3826 (2014).

[32] W.S. Chiu, P.S. Khiew, M. Cloke, D. Isa, T.K. Tan, S. Radiman, R. Abd-Shukor, M.A. Hamid, N.M. Huang, H.N. Lim, C.H. Chia; Chemical Engineering Journal **158,** 345 (2010).

[33] G. Zheng, W. Shang, L. Xu , S. Guo, Z. Zhou; Materials Letters **150,** 1 (2015).

[34] N. Kaneva , I. Stambolova, V. Blaskov, Y. Dimitriev, A. Bojinova, C. Dushkin; Surface and Coatings Technology **207,** 5 (2012).

[35] P.W. Fan, W.L. Chen, T.H. Lee, Y.J. Chiu, J.T. Chen; Macromolecules **45,** 5816 (2012).

[36] C. Busuioc, A. Evanghelidis, C. Florica, I. Enculescu; Digest Journal of Nanomaterials and Biostructures **9,** 1569 (2014).

[37] A. Aravind, M.K. Jayaraj, M. Kumar, R. Chandra; Applied Surface Science **286,** 54 (2013).

[38] W.K. Tan, G. Kawamura, H. Muto, K.A. Razak, Z. Lockman, A. Matsuda; Journal of Luminescence **158,** 44 (2015).

[39] G. Srinet, R. Kumarn, V. Sajal; Ceramics International **40,** 4025 (2014).

[40] O. Mekasuwandumrong, P. Pawinrat, P. Praserthdam, J. Panpranot; Chemical Engineering Journal **164,** 77 (2010).